Main Manuscript for

Urban tree deaths from invasive alien forest insects in the United States, 2020-2050.

Emma J. Hudgins[1], Frank H. Koch[2], Mark J. Ambrose[3], Brian Leung[1,4]

[1] Dept. of Biology, McGill University

[2] USDA Forest Service, Southern Research Station

[3] Dept. of Forestry and Environmental Resources, North Carolina State University

[4] School of Environment, McGill University

*Corresponding author: Emma J. Hudgins.

Email: emma.hudgins@mail.mcgill.ca

Author Contributions: EJH and BL conceptualized the study. EJH performed the analyses and created the figures. EJH, BL, FHK and MJA wrote the paper. FHK and MJA provided insect and urban tree expertise and commented on realism of results. MJA manages the urban tree database.

Competing Interest Statement: The authors have no competing interests to disclose.

Classification: Biological Sciences: Ecology; Social Sciences: Environmental Sciences

Keywords: Forest ecology, Economic impact, Scenario modelling, Invasive species

This PDF file includes:

Main Text
Figures 1 to 4
Tables 1 to 1

Abstract

With 70% of the global population in urban centers, the 'greening' of cities is central to future urban wellbeing and livability. Urban trees can be nature-based solutions for mental and physical health, climate control, flood prevention and carbon sequestration. These ecosystem services may be severely curtailed by insect pests, which pose high mortality risks to trees in urban centers. Until now, the magnitudes and spatial distributions of mortality risks were unknown. Here, we combine new models of street tree populations in ~30,000 United States (US) communities, species-specific spread predictions for 57 invasive insect species, and estimates of tree death due to insect exposure for 48 host tree genera. We estimate that an additional 1.4 million street trees will be killed by insects from 2020 through 2050, costing an annualized average of US$ 30M. However, these estimates hide substantial variation: 23% of urban centers will experience 95% of all insect-induced mortality, and 90% of all mortality will be due to emerald ash borer (*Agrilus planipennis*, EAB). We define an EAB high-impact zone spanning 902,500km^2, largely within the Midwest and Northeast, within which we predict the death of 98.8% of all ash trees. "Mortality hotspot cities" facing costs of up to US$ 13.0 million each include Milwaukee, WI, Chicago, IL, and New York, NY. We identify Asian wood borers of maple and oak trees as posing the highest future risk to US urban trees, where a new establishment could cost US$ 4.9B over the same time frame.

Significance Statement

US urbanization levels are already at 82% and are growing, making losses of ecosystem services due to urban tree mortality a matter of concern for the majority of its population. To plan effective mitigation, managers need to know which tree species in which parts of the country will be at greatest risk, as well as the highest-risk insects. We provide the first country-wide, spatial forecast of urban tree mortality due to invasive insect pests, including forecasts for each host tree and each insect species in each US community. This framework identifies dominant pest insects and spatial hotspots of high impact. Further, these findings produce a list of biotic and spatiotemporal risk factors for future high-impact US urban forest insect pests.

Main Text

Introduction

Previous analyses suggest that impacts associated with urban trees are likely to comprise the dominant share of economic damages caused by invasive alien forest insects (IAFIs) in the United States (US) [1]. Urban tree populations include highly susceptible species like ash (*Fraxinus spp.*) that are being decimated by emerald ash borer (EAB, *Agrilus planipennis*) [2]. To eliminate the potential for injury or property damage due to dead trees, infested urban trees must be treated or removed [3]. Moreover, the importance of urban forests is only expected to grow. While urbanization is already very high in the US (82% in 2018), it has not yet reached saturation (World Bank, http://data.worldbank.org, UN DESA, http://population.un.org). At the same time, there has been a push for urban 'greening' (i.e., increasing urban forest canopy). Urban trees perform many important ecosystem services, including lowering cooling costs [4], buffering against flooding, increasing air quality, carbon sequestration, improving citizens' mental and physical health outcomes, and creating important habitat [5,6]. The high tree mortality risk posed by IAFIs can greatly diminish these myriad benefits.

While IAFI life histories differ, they are known to be transported long distances by humans [7], potentially with similar drivers across entire dispersal pathways [8]. Thus, the creation of a pathway-level damage estimate can provide insight into the benefit of limiting future spread via these pathways (e.g. through quarantines, highway checkpoints to limit firewood

movement). Past estimates of IAFI damage have been important in providing support for phytosanitary measures such as ISPM15 [10], a wood packing material treatment protocol, whose adoption is growing worldwide [11]. A previous pathway-level estimate for the cumulative cost of all US IAFIs was performed a decade ago and had substantial data limitations [1]. Since then, contemporary advances allow direct estimates of spread for every IAFI species as well as host prevalence and IAFI-induced mortality for every tree species in every community across the United States. This allows not only the estimation of country-wide IAFI damages, but also IAFI and host-specific damages and their spatial distribution. Further, we can examine the impact of tree mortality dynamics on cost dynamics, and derive better risk assessments of not-yet established pests, based their functional traits and host distributions.

In this paper, we synthesized four subcomponent models of IAFI invasions: 1) a model of 57 IAFI species' spread, 2) a model for the distribution of all urban street tree host genera across all US communities, 3) a model of host mortality in response to IAFI-specific infestation for all urban host tree species, and 4) the cost of removing and replacing dead trees, to provide the best current estimate of the damage to street trees, including explicit estimates for all known IAFIs across all major insect guilds (Fig. S1-S2).

Results

Urban tree pest exposure

Total tree abundance models were predictive with some outliers (Appendix S1, Fig. S4, small trees: R^2 = 0.78, medium trees: R^2 = 0.58 large trees: R^2= 0.42). Removing the outliers changed the R^2 to 0.76 for small trees, 0.76 for medium trees, and 0.58 for large trees. Our genus-level abundance models were strong but became slightly weaker for rare genus - size class combinations (Fig. 1, overall R^2 for all genera of small trees: R^2= 0.93, medium trees: R^2 = 0.93, large trees: R^2 = 0.92). While relationships were variable across genera, the genera that were fit most poorly did not make up a large proportion of predicted trees, and none were below R^2 = 0.25 (Fig. S5).

We tested four model types (global BRT, global GAM, customized BRT, or customized GAM) to fit 1) genus-level tree presence/absence and 2) genus-level abundance models (Fig. S1). The optimal genus-level fitting approach differed across genera depending on diameter class, prevalence of genera, and whether presence/absence or tree abundance was the response variable (Table S2). Generally, rarer genera were better fit by global BRT and GAM models, which utilized information from all other species while common species were better fit by customized models (Fig. S6). According to our models, while subject to regional variation, the population of street trees is mostly made up of maple (*Acer*) and oak *(Quercus)*, with substantial ash (*Fraxinus,* Fig. S7).

We analyzed street trees separately from residential and community trees. Predicted street tree exposure (measured as the number of predicted susceptible trees in Fig. 2a * IAFI relative propagule pressure in Fig. 2b, [8]) across all tree types from 2020 to 2050 was generally high in the eastern US, and only sporadically high across the western US (Fig. 2c). Predicted street tree exposure was highest among maples (*Acer* spp*.,* 25.6M predicted exposed trees), oaks (*Quercus* spp*.,* 5.9M), and pines (*Pinus* spp. 3.4M). The greatest number of trees were predicted to become exposed to Jose scale (*Quadraspidiotus perniciosus*, 7.3M), Japanese beetle (*Popillia japonica*, 6.7M), calico scale (*Eulecanium cerasorum*, 6.4M), San. Among residential and community trees, exposure was greatest among maples, oaks, and *Prunus* spp. (1.7B,1.1B, 707M, respectively), and the most frequently predicted IAFI encounters were with the same three species (Japanese beetle, San Jose scale, and calico scale).

Host tree mortality

The best-fitting mortality model indicated that most IAFIs fall in the low severity groups. Within all severity groups, the majority of IAFIs were at the low end of severity (Fig. 3, full results in Appendix S2). We define the term 'mortality debt' as the time period between an IAFI initiating damage within a community and reaching its estimated asymptotic host mortality within that

community (*see Methods*). In our most likely mortality debt scenario (i.e., 10-year scenario for borers, 50-year scenario for defoliators, 100-year scenario for sap feeders), we estimated a mortality level of 0.7-2.5% beyond expected natural mortality of street trees by 2050, where our most likely scenario fell on the higher end of this range (Table 1). Predicted street tree death varied by a factor of four based on the mortality debt scenario, with longer debts leading to lower total mortality between now and 2050 (Table 1). This was because in longer mortality debt scenarios, trees experience mortality in the years 2020-2050 from IAFIs that initially established in their communities in 2000 (50yr debt) or 1950 (100yr), but our highest impact IAFI (EAB) can only begin to cause mortality after 2002 in any scenario. Sensitivity was driven largely by wood boring species, as demonstrated by the sensitivity of mortality estimates to their mortality debt scenarios ("Vary Borers" row, Table 1). We also found that longer mortality debts lead to a smoother cost curve, or costs that do not vary much due to more consistent host mortality rates (Fig. 4).

Spatially, future damages will be primarily borne in the Northeast and Midwest, driven by EAB spread (Fig. 2d). We predict that EAB will reach asymptotic mortality in 6747 new cities, which means that 98.98% of its preferred *Fraxinus* spp. hosts will die. Thus, the mortality is predicted to be concentrated in a 902,500km^2 zone encompassing many major Midwestern and Northeastern cities (Fig. S10). This mortality is also predicted to result in a 98.8% loss of all ash street trees within this zone. Over 230,000 ash street trees are predicted to have died before 2020, and there are a further 69 cities where EAB is predicted to reach asymptotic mortality within 10 years of 2050 (i.e., 98.8% ash mortality by 2060). Due to the restricted range of forest ash relative to urban ash, we predict that 68% of ash trees and 76% of communities containing street ash will remain unexposed to EAB in 2060. Furthermore, at-risk ash trees are unequally distributed. We projected the highest risk close to the leading edge of present-day EAB distributions, particularly in areas predicted to have high ash densities. The top "mortality hotspot cities", where projected added mortality is in the range of 5,000-25,000 street trees, include Milwaukee, WI, the Chicago Area (Chicago/Aurora/Naperville/Arlington Heights, IL), Cleveland, OH, and Indianapolis, IN (Fig. 2d). Cities predicted to have high mortality outside of the Midwest include New York, NY, Philadelphia, PA, and Seattle, WA – communities with high numbers of street trees and high human population densities, which attract EAB propagules within our spread model. The states most impacted by street tree mortality match these patterns, where the highest mortality is predicted for Illinois, New York, and Wisconsin.

Cost estimates

We estimated annualized street tree costs across all guilds to be between US$29-33M per year in our most likely scenario (mean = $30M, Table 1). Roughly 90% of all costs across the entire US were due to EAB-induced *Fraxinus* spp. mortality. The total cost associated with street tree mortality in the top ten hotspot cities was estimated at $50M from 2020 to 2050, with $13M in Milwaukee, WI alone.

The ranking of feeding guild severity was relatively robust across mortality debt scenarios, in spite of the potential for differences due to the interaction of IAFI-specific spread and mortality debt dynamics. Costs were higher for longer mortality debt scenarios for borers, peaked at intermediate debt for defoliators, and peaked at the longest debt for sap feeders. These patterns were due to the relative rates of historical and contemporary range expansion of more impactful IAFIs (i.e. high impact borers have more rapid recent range expansion, while contemporary high impact defoliator expansion is slow compared to 50 years ago). Borers were predicted to be the most damaging feeding guild ($8M-28M mean annualized street tree damages across scenarios), and EAB was consistently the top threat. Defoliators were predicted to be the second most damaging feeding guild in the next 30 years (means = $0.8M-$1.4M), in spite of more widespread hosts than wood borers, due to lower asymptotic mortality levels. Defoliators had a 1-2 order of magnitude lower cost than wood-boring species, but again showed consistency in which species were the top threats within the guild. Consistent with previous work in [1], European gypsy moth had the highest cost of all defoliators, followed by Japanese beetle and cherry bark tortrix (*Enarmonia formosana*). The sap-feeding group accrued the lowest costs

in the next 30 years due to their lower asymptotic mortality and rarer street tree hosts (mean = $0.2M-1.1M). Hemlock woolly adelgid (*Cryptococcus fagisuga*) was the highest impact sap feeder, followed by oystershell and elongate hemlock scale insects (*Lepidosaphes ulmi, Fiorinia externa*). Total costs were only notably sensitive to borer mortality debt scenario misspecification (Table 1), which is promising, given our certainty of the shorter scenario for EAB.

Potential impacts to non-street trees

Mean added mortality (i.e. above background rates) for residential and non-residential community trees in the most likely scenario was 1.0% (13.3M residential and 72.1M non-residential trees, Table S10). While recognizing that non-street tree management will likely be more variable, to provide a rough estimate, we assumed that non-street trees would be managed in the same way as street trees (i.e. removal and replacement of dead trees). In this scenario, added mortality would incur an estimated annualized cost of $1.5B for non-residential trees and $356M for residential trees. Further, a disproportional amount of the total damages (91% of the mortality to residential non-residential community trees) is expected to be felt in the aforementioned hotspot zone, with 12.1 million residential and 65.9 million non-residential community trees expected to be killed. Given the relatively limited data, and the difference in potential management behaviour for these trees, we caution against overinterpretation of these results.

Novel IAFI risk forecast

Our framework allowed us to identify the factors leading to the greatest impacts for IAFIs already known to have established in the United States. We were able to identify the most common urban host trees, the sites facing the greatest future IAFI propagule pressure, and the IAFI-host combinations with the greatest mortality. However, this approach can also be synthesized with IAFI entry scenarios to understand potential impacts of novel invasive IAFIs. To illustrate the utility of this framework predictively, we have provided a checklist of risk factors in Table S11 and future spread simulations in Table S12 and Fig. S12. We show that entry via a southern port (e.g. the Port of South Louisiana) would lead to the greatest number of exposed trees. Further, an EAB-like borer of oak and maple trees could kill 6.1 million street trees and cost $4.9B over the next 30 years.

Discussion

While previous analyses have indicated that urban trees are associated with the largest share of economic damages due to IAFIs [1,13,14], until recently, data did not exist on the urban distribution of host trees [15], the spread of IAFIs [8], nor the mortality risk for hosts due to different IAFIs [16]. With these new models, it is now possible to forecast where and when IAFIs will have the most damages across the US. Our analysis suggests an overall added mortality of between 2.1-2.5% of all street trees, amounting to $US 30M per year in management costs. However, the most interesting and potentially useful element was our ability to forecast hotspots of future forest IAFI damages, including a 902,500km^2 region that we expect to experience 95.7% of all mortality, in large part due to a 98.8% loss of its ash street trees due to EAB. This type of forecasting has been highlighted as a crucial step in prioritizing management funds [17]. These data can be used by municipal pest managers to anticipate future costs, and may help motivate improved spread control programs that aim to identify the potential source counties of future invasions and mitigate the worst anticipated impacts (complete forecast available at http://github.com/emmajhudgins/UStreedamage).

Beyond present IAFI risks, our integrated model can also act as a risk assessment tool for street tree mortality caused by novel IAFIs (Table S11-S12, Fig. S12). While ash trees are assured to be dramatically affected by EAB over the next few decades, our models suggest oak and maple to be the most common street tree genera nationwide. Further, while ash species are being substituted for less susceptible tree species, maples and oaks continue to be widely planted within our street tree inventories. Therefore, IAFIs with host species spanning these

genera should be of heightened concern. Secondly, the timescale and magnitude of the impacts of wood borers (see also [1]) make them the highest risk to street trees. We integrated these two pieces of information with information on major ports of entry within the US (American Association of Port Authorities 2015, http://aapa.com/), as well as our general model of IAFI spread [8], to forecast the extent of exposed maple and oak street trees from 2020-2050 (Fig. S12, Table S12). Our analyses show that entry via a southern port would lead to the greatest number of exposed trees. Further, larger trade volumes between the US and Asia compared to other regions [18] suggest Asian natives will be the most likely future established IAFIs. One potential candidate species fitting these criteria is citrus longhorned beetle, which is an Asian wood borer thought to have many potential host species within the United States, including ash, maple and oak [19]. The lack of strict implementation of current wood treatment protocols such as ISPM15 [20] increases the susceptibility of the US to invasion and subsequent spread of this species and other potentially high-risk borers.

Our impact estimates vary substantially based on dynamics of host mortality following initial IAFI invasion, especially because of variability in the duration and functional form of mortality debt. Luckily, the guild (borers) and species (EAB) whose impact on total community costs are most sensitive to correct specification of the mortality debt dynamics are the ones for which we are most confident. Several publications have demonstrated near-complete decimation of ash stands in the decade following EAB infestation [2,21,22]. Furthermore, since total tree mortality is asymptotically equivalent across all mortality debt regimes, if other feeding guilds possessed 10-year mortality debt regimes, we should have been able to detect a rapid die-off of their hosts as they spread, similarly to what we found for EAB (albeit scaled by their maximum mortality rates). This is not the case in the literature [22].

With our integrated model, we also estimated economic damages, which updates the decade old Aukema et al. [1] using recent advances [13,14]. Surprisingly, the previous cost estimates were not that different at the country scale. The previous cost estimate separated urban trees into residential and non-residential types (grouping street trees in the latter). We estimate annualized costs for non-residential trees to be somewhat lower than those in [1] ($1.3B versus $2.0B in total “Local Government expenditures”). This lower estimate is likely because of a lower rate of predicted *Fraxinus* exposure to EAB (i.e., lower predicted ash abundance in areas of predicted EAB spread) in non-residential areas. Interestingly, our estimate of residential tree costs is roughly one third that in [1] ($303M vs $1.1B in total “Household Expenditures”), again likely due to a (more extreme) overestimate in the nationwide prevalence of residential ash trees in the previous publication.

Additionally, we predict that 75% of communities containing ash trees and 68% of all street ash will remain untouched by EAB by 2060 because of the lack of forest ash beyond our forecasted invasion extent (i.e., affecting exposure). However, in some EAB infested communities, it is important to note that our street tree distributional model may overestimate the tree mortality projected, due to the role of preventative cutting prior to EAB arrival, which occurred in many cities across IN, IL, MI, and WI. Preventative cutting would have led to the payment of tree removal costs prior to our estimation window. This is particularly likely to have inflated the 2020-2050 costs to communities with large street tree budgets in regions where EAB was predicted to invade in the years 2010-2020 (therefore initiating mortality 2020-2030).

Spatially, our results show clear patterning of high threat in the eastern and central US, and lower threat in the western US. This pattern is consistent with previous findings [20], and can be explained by the high impacts of EAB, European gypsy moth, and hemlock woolly adelgid, whose distributions are projected to concentrate further east in the short term. However, some of the highest-impact non-native pathogens have emerged in the western US, and were not captured in this analysis [23,24]. Western regions could also see high future risks due to the polyphagous shot hole borer (*Euwallacea whitfordiodendrus)*, and its insect-disease complex with fusarium fungus (*Fusarium spp.*) [25]. This complex has already established in California and has maple and oak trees among its many hosts.

While the substantial advances that emerged recently allowed us to develop a more fully integrated model, we also identified data deficiencies which require additional research. A relative

quantification of additional sources of uncertainty is provided in Appendix S3. This cost estimate is arguably a lower bound, since it only examines the cutting of dead trees. The analysis also fails to account for preventative management, to fully examine non-street tree management, and to assess the impacts of IAFIs that have not yet established in the United States. Furthermore, our analysis assumes a complete identification of 'high impact IAFIs'. Some presently established US may not yet have been identified as 'high impact', either due to lags in their impact, and/or lags the detection of this impact [26], but may achieve the same level of recognition as those in [1] before 2050.

Conclusion

We have shown that the suite of known IAFIs have the potential to kill roughly a hundred million additional urban trees in the US in the next 30 years. While these numbers themselves are striking, reporting only a country-level impact estimate without IAFI species, tree, and community-level resolution does little to inform management prioritizations. Here, we were able to identify specific urban centers, IAFI species, and host tree genera associated with the vast majority of these impacts. We predict that 90% of all street tree mortality within the next 30 years will be EAB-induced ash mortality, and that ~95% of all street tree mortality will be concentrated in less than 25% of all communities. These estimates illustrate the gravity of IAFI infestations for communities in the path of high impact invaders that are rich in susceptible hosts. Further, we were able to use this framework to identify a checklist of biotic and spatiotemporal risk factors for future high-impact street tree IAFIs.

Materials and Methods

We synthesized four subcomponent models of IAFI invasions: 1) a model of 57 IAFI species' spread, 2) a model for the distribution of all urban street tree host genera across all US communities, 3) a model of host mortality in response to IAFI-specific infestation for all urban host tree species, and 4) a simple model of the human management response to dead host trees, to provide the best current estimate of the damage to street trees (see conceptual diagram, Fig. S1).

IAFI dispersal forecasts

We modelled spread using the Semi-Generalized Dispersal Kernel (SDK, [8]). This is a spatially explicit, negative exponential dispersal kernel model that can account for additional spatial predictors in source and recipient sites. The SDK builds from the Generalized Dispersal Kernel (GDK, [8]) as a starting point, using human population density, forested land area and tree density in source and destination sites as moderators of spread. The SDK combines up to three species-specific corrections for each species to maximize predictive ability: 1) a species-specific intercept term, 2) information on an IAFI's likely initial invasion location, and 3) niche-related limitations when evidenced in the literature. The SDK was applied to all 57 IAFIs believed to cause some damage from [1], and projected from 2020 to 2050 (Fig. S2).

Street tree models

Our fitting set consisted of 653 street tree databases for US communities where street tree inventory data had been collected (Fig. S3, [14]). In two communities (Tinley Park and, IL and Fort Wayne, IN), preventative cutting for EAB was conducted prior to the most recent inventory and was therefore accounted for within our dataset. We modelled the abundance and diameter at breast height (DBH) for trees within each genus, as treatment costs are dependent on number and diameter of trees [1]. We split trees into three diameter classes (small = 0-30cm, medium = 31-60cm, large >60cm). We first fit models for the total tree abundance of all species by diameter class, and then used these total tree models to help predict genus-specific tree abundance within each diameter class. Street tree inventory data are not always reliably reported to the species level across municipalities, and some species are so rare in street tree inventories that it would have been very difficult to develop robust species-level models, so we limited our examination to the genus level. Since IAFIs may not be equally impactful to all host tree species in a genus, we

had to estimate the genus-level severity of each IAFI species for each IAFI-host combination. We did so by estimating the species-level breakdown of each genus based on their average relative proportions across our 653 inventoried communities, and assuming this distribution was representative in other projected communities.

We modelled the total abundance of street trees in a community using boosted regression trees (BRT, *gbm.step* within R package *dismo,* [27]) relating the logarithmically-scaled total tree abundance within a diameter class to community-specific predictors, employing environmental variables from WORLDCLIM [28] and community characteristic s used in [13], and sourced largely from the National Land Cover Database (NLCD,[29]), the US Census and the American Community Survey (https://www.census.gov/data.html, Table S1). We hypothesized that the age and wealth of a community would influence the types and sizes of trees planted there. In our model, median home value and mean year of construction (at the block-group level) as well as median household income (at the county level) were used as proxies of the age of the urban tree community and the community budget for street trees. We also tested the use of Poisson GAM models, but high levels of concurvity (the GAM equivalent of multicollinearity, [30]) amongst predictors and lower predictive performance indicated Poisson GAMs were an inferior modelling structure for estimating total abundance.

Next, we estimated the abundance of street trees within each genus, using the same climatic and demographic factors as the total tree abundance model as well as the total tree abundance model output as predictors (Fig. S1). We considered two approaches: 1) Zero-inflated Poisson GAMs, or 2) a two-step BRT approach. For BRT, we modeled tree presence/absence, followed by tree abundance given presence (using logarithmically-scaled tree abundance and back-transforming when predicting), and then combined the two models. The number of trees of genus *i* in size class *j* at a particular site *k* was:

$$trees_{i,j,k} = c_{i,j,k} * pred_{exist,i,j,k} * pred_{number,i,j,k} \quad (1)$$

$$c_{i,j,k} = \frac{1}{\sum_k (pred_{exist,i,j,k} * pred_{number,i,j,k}) / \sum_k obs_{number,i,j,k}} \quad (2)$$

This process is similar to a zero-inflated Poisson (ziP) model [31] but does not link the parameters of the binary and continuous components of the model, instead fitting them separately. Because our BRT approach was built from two independent parts, we needed to add a rescaling step so that the output summed to the observed counts (eqn. 2), as occurs for ziP models by default [31]. We removed all highly correlated variables ($r > 0.8$) prior to fitting, and refit GAMs until maximum estimated worst-case concurvity using three-knot smoother functions was below 0.8 (*concurvity* function within *mgcv,*[32]).

We compared BRT and GAM models that were fit to all genera simultaneously (general BRT/GAM models using genus-specific intercept terms) with models that were fit to each genus separately (customized BRT/GAM models) (Fig. S1). Predictive power could be higher when modelling all genera together if the genera respond similarly to predictors, while power could be higher for individually fitted genera where environmental and community characteristic relationships are idiosyncratic and where the sample is sufficiently large.

We chose the model that produced the strongest relationship for each genus using R^2 values that were relative to the 1:1 line (i.e, a normalized mean squared error, R^2_{MSE}). R^2_{MSE} more correctly measures deviations between observations (y) and predictions ($\hat{y}$) than conventional R^2.

$$R^2_{MSE} = 1 - \frac{\sum (y-\hat{y})^2}{\sum (y-\bar{y})^2} \quad (3)$$

We removed New York, NY from the fitting set as it was likely to be a high leverage observation and could have significantly changed the resulting models due to it possessing a markedly different street tree genus composition from all other communities. Both the GAM and BRT models were fitted using their built-in cross-validation algorithms for parameter estimation, and can therefore tolerate occasional outliers with minimal effect on their parameter estimates (though we have less evidence that other outliers would have changed model parameters for cities other than New York, NY). Given the higher data requirements of GAMs (i.e. all parameters must be fit simultaneously, rather than BRT, which can fit subsets of predictors to each tree, [33]), genus-specific GAMs were not considered when data were insufficient (i.e., when only a few cities

contained that genus). For each genus, we used the best-fitting model to predict urban tree distributions throughout the contiguous US. We used the observed number of trees rather than model predictions in cities where these data were available. Alaska and Hawaii were removed to match the spatial extent of IAFI spread predictions, and because urban tree genus composition is likely quite different in these areas compared to the contiguous US.

We synthesized the previous two modelling steps, intersecting IAFI spread forecasts with predicted tree distributions (using observed tree data where available), to create forecasts of tree exposure, which we define as the sum of predicted density of each IAFI species, multiplied by their predicted host tree abundance in each community.

Host mortality model

We examined the impacts of the three major feeding guilds of IAFIs [34]: Foliage feeders included insects that feed on leaf or needle tissue. Sap feeders included all species that consume sap, including scale insects and gall-forming species. Borers included species that feed on phloem, cambium, or xylem. Across insect guilds, the logic from [1] appeared to hold: most species were innocuous, but a small number caused high mortality (Table S7). In contrast, while several invasive pathogens were mentioned in [14], pathogens are only reliably reported when they produce noticeable (i.e. intermediate) impacts [1]. To avoid mischaracterizing their impacts, we removed pathogens from the remainder of our analysis.

We ranked the severity of a given IAFI infestation on a particular host using a scale based on observed long-term percent mortality (defined in [14], Table S7). We added two additional categories to this scale to represent IAFI species missing from their database that are still considered pests on a particular host in [1]. The lowest-impact IAFI-host combinations were those featuring IAFIs reported as 'low impact' in [1]. These accounted for most known combinations. The second lowest category featured 'intermediate impact' IAFI species from [1] that did not appear as threats to a given known host in [14]. We assumed that, were these species quantified by [14], their associated severities would be lower than the lowest category within the authors' ranking scheme. All other IAFI-host combinations were assigned to the same categories as in [14]. IAFI frequency within severity categories was normalized across the sum of their known hosts so that each IAFI had equal impact on the frequency distribution (i.e., frequency summed to 1 for each IAFI). For instance, if an IAFI had 3 hosts, and had severities of 3, 5, and 9 on each host, we would give them a frequency of 1/3 under each bin. We fit a Beta distribution to the frequency distribution of IAFIs in each of these categories using Stan [35], a program and language for efficient Bayesian estimation. We chose to fit a Beta distribution because proportional mortality ranged between 0 and 1. Additionally, we fit the upper limit of the two lowest mortality categories and the lower limit of the highest category, as these categories did not have quantified bounds, but could be ranked relative to others. We used the posterior mean as the expected mortality for an IAFI in each severity category, rather than the simple midpoint of the range of each category.

We define the term 'mortality debt' as the time period between an IAFI initiating damage within a community and reaching its estimated asymptotic host mortality within that community. While we had estimates of the asymptotic proportional mortality of host trees [14], we had no information on the rate by which trees reach this plateau. Previous estimates have ranged from 5 to 100 years [1,36], so we analyzed three scenarios within this range (10, 50, 100 years). To account for what is currently known about the mortality dynamics of IAFIs within each of the feeding guilds, we also examined scenarios based on our most likely scenario of the duration of mortality debt across IAFI feeding guilds. EAB is estimated to kill the majority of its susceptible hosts in the first decade following infestation [19], while maximum mortality is estimated to take closer to 100 years for hemlock woolly adelgid [1], so we used the 10 and 100-year scenarios for borers and sap-feeders, respectively. A recent publication examining mortality rates in forested areas suggested that European gypsy moth has a mortality rate intermediate between borers and sap-feeders, so we set defoliators at 50-years [20]. Once an IAFI was predicted to infest an area, we imposed a 10-year initial lag phase between IAFI arrival at a site and the initial onset of damage [37,38] and then began increasing the host mortality following our mortality debt scenario

to the asymptotic level (defined by the host mortality model). For simplicity, we assumed mortality increased by a constant fraction over time until reaching its maximum and levelling off. For example, in the 50-year mortality debt scenario, if an IAFI's maximum host mortality was defined as 90%, mortality would increase by 9% at each 5-year timestep for 10 timesteps until 90% mortality had been reached.

The joint impact of maximum mortality and mortality debt is best illustrated by a series of examples. Estimates of street tree natural mortality range around 2.4-2.6% per year [12]. Within a 30-year window, this would amount to roughly 53% natural street tree mortality. Our model assumes that if IAFI enters site at the beginning of this window (2020), it first undergoes a 10-year time lag, and can then cause mortality in the final 20 years. The maximum level of mortality induced by a borer (EAB on several *Fraxinus* spp., Category H = 98.98%), would result in 98.98% additional mortality (mortality of remaining the trees that survived natural mortality) at the end of a 30-year window. This level of mortality would be clearly detectable above natural street tree mortality. Hemlock woolly adelgid has a similar maximum mortality to EAB (Category H on *Tsuga* spp.), but we have assumed that sap-feeder mortality takes 100 years to reach asymptotic levels. As such, by the end of a 30-year window, only (98.98%/100)*20 years = 19.80% of additional host trees would be killed. While defoliators have shorter mortality debts, they tend to cause lower mortality, making their impacts the least detectable above background mortality. For defoliators, the IAFI with the greatest damage on any host is the larch casebearer, (*Coleophora laricella* on *Larix laricina*, category E = 16.46%). Given a 50-year mortality debt for defoliators, the maximum mortality above background rates by 2050 is (16.46% / 50) * 20 years = 6.58%. While these estimates are much lower, many host trees of sap feeders and defoliators are very common, and this mortality could very well be inflating the perceived background mortality rates of these host trees measured in [12].

Management costs

As a final layer that allowed us to move from mortality estimates to cost estimates, we estimated the cost of removing and replacing dead trees. We used this cost because we believe it to be the minimum management response required, and because the extent and variability of preventive behaviour would be much harder to estimate. However, we note that this cost does not account for additional preventive cutting or any non-cutting management such as spraying or soil drenching with pesticides. We assumed that cutting was a one-time 100% effective treatment against IAFIs, or in other words, that newly planted trees were of different species and thus not susceptible to the same IAFI species that killed the previous trees. We assumed a 2% discount rate for future damages [1] and also that infestations were independent, or in other words that invasion by one IAFI did not interfere with invasion by another. This is likely a fair assumption, as there is minimal host sharing across IAFIs, and IAFI species each infest only a small proportion of hosts at a given time interval, so there is minimal potential for species interactions [30]. We assumed the same per-tree cost estimates for cutting and replacing dead trees as in [1], where the cost of cutting increases nonlinearly with size class. If we assume that street trees are always under the jurisdiction of local governments, the cost of removal and replacement of each tree is US$450 for small trees, US$600 for medium trees, and US$1200 for large trees (these costs jump to an estimated US$600, US$800, and US$1500 for homeowners). We reported all costs incurred from 2020 to 2050 in 2019 US dollars based on a 2% discount rate relative to these baseline costs. Since these baseline per-tree management costs came from a 2011 publication, we converted them to 2019 dollars via the consumer price index, which amounted to an inflation of 13.65% (World Bank, https://data.worldbank.org), though we note that the present-day costs of per-tree removal may have declined with advances in technology.

Model synthesis

Once all subcomponent models had been parameterized, we synthesized the street tree estimates, IAFI spread estimates, host mortality estimates, and removal costs to produce overall cost estimates (Fig. S1). We summed the damages from 2020 to 2050 to obtain a total

discounted cost for this 30-year window. We then obtained annualized costs by calculating an annuity over the 30-year time horizon using the following equation:

$$Annualized\ damage = D\frac{\sum_{time=min}^{max} Costs_{time}}{(1-(1+D)^{min-max})} \quad (4)$$

Where D is the discount rate (2%). Using these forecasts, we extended the concept of cost-curves from [1], which were based on frequencies of occurrences of low and intermediate damaging IAFI, and explicit economic estimates of three 'poster pests'. To parameterize the cost-curves in this manuscript, rather than just 3 poster pests, we estimated street tree costs for all 57 intermediate-impact IAFIs across the 3 major insect feeding guilds, in addition to frequencies of low-impact species (Table S4.1). The summed area under each guild-specific curve can be interpreted as the estimate of the total annualized cost of all IAFIs in the US to street trees. Since our curves were missing only low-impact species, the total cost estimated with these approaches is not appreciably different from a simple sum of the costs of the non-missing (57 intermediate) species reported in text, but we included these analyses to allow for the prediction of the costs of novel invaders from each guild (Appendix S4).

We assessed parameter uncertainty in proportional host mortality by sampling from our posterior beta mortality distribution. We also used sensitivity analysis to explore the effect of different mortality debt scenarios, including 1) our most likely scenario, 2) setting all guilds to 10, 50, or 100-year debts, and 3) varying each guild separately while holding the other two guilds at their most likely scenario. While our host distribution models were based on standard modelling approaches (e.g. GAM), our Bayesian formulations underlying the mortality estimates were novel and needed to be tested theoretically, to ensure that parameters were identifiable, and reproduced the correct behavior. See Appendix S4 for details of our theoretic analyses.

Potential impacts to non-street trees

To provide a rough estimate of non-street tree impacts, we built a model for whole-community trees (i.e., street + non-street trees) from the dataset of 56 communities where genus-level estimates were reported, subtracted predicted street trees from this whole community estimate, and apportioned the remaining trees into residential and non-residential trees based on their average fractions across all sites where land type breakdowns were provided (32 municipalities). Given the relatively limited data, we caution against overinterpretation of these results.

Acknowledgments

EJH would like to thank her PhD supervisory committee members T. Jonathan Davies and Patrick M. A. James for their invaluable comments, as well as the thoughtful comments and questions from thesis external examiner Dominique Gravel and colleague Andrew Liebhold. EJH also acknowledges the continual support and feedback from lab members Dat Nguyen, Abbie Gail Jones, Charlotte Steeves, Shriram Varadarajan, and Lidia Della Venezia. This work was supported by a NSERC CGS-D awarded to EJH.

References

1. Aukema, J. E., Leung, B., Kovacs, K., Chivers, C., Britton, K. O., Englin, J., ... *et al.* (2011). Economic impacts of non-native forest insects in the continental United States. *PLoS One,* 6(9).

2. Kovacs, K. F., Haight, R. G., McCullough, D. G., Mercader, R. J., Siegert, N. W., & Liebhold, A. M. (2010). Cost of potential emerald ash borer damage in US communities, 2009–2019. *Ecological Economics*, 69(3), 569-578.

528 3. Fahrner, S. J., Abrahamson, M., Venette, R. C., & Aukema, B. H. (2017). Strategic
529 removal of host trees in isolated, satellite infestations of emerald ash borer can reduce
530 population growth. *Urban Forestry & Urban Greening*, *24*, 184-194.

531 4. Norton, B. A., Coutts, A. M., Livesley, S. J., Harris, R. J., Hunter, A. M., & Williams, N. S.
532 (2015). Planning for cooler cities: A framework to prioritise green infrastructure to mitigate
533 high temperatures in urban landscapes. *Landscape and Urban Planning*, 134, 127-138.

534 5. Van den Berg, A. E., Maas, J., Verheij, R. A., & Groenewegen, P. P. (2010). Green space
535 as a buffer between stressful life events and health. *Social science & medicine*, 70(8),
536 1203-1210.

537 6. Roy, S., Byrne, J., & Pickering, C. (2012). A systematic quantitative review of urban tree
538 benefits, costs, and assessment methods across cities in different climatic zones. *Urban*
539 *Forestry & Urban Greening*, 11(4), 351-363.

540 7. Hulme, P. E. (2009). Trade, transport and trouble: managing invasive species pathways
541 in an era of globalization. *Journal of Applied Ecology*, *46*(1), 10-18.

542 8. Hudgins, E. J., Liebhold, A. M., & Leung, B. (2017). Predicting the spread of all invasive
543 forest pests in the United States. Ecology letters, 20(4), 426-435.

544 9. Hudgins, E. J., Liebhold, A. M., & Leung, B. (2020). Comparing generalized and
545 customized spread models for nonnative forest pests. Ecological Applications, 30(1),
546 e01988.

547 10. IPPC (International Plant Protection Convention). 2002. International standards for
548 phytosanitary measures. Rome, Italy: FAO.
549 www.fao.org/docrep/009/a0450e/a0450e00.htm. Viewed 12 May 2020.

550 11. Leung, B., Springborn, M. R., Turner, J. A., & Brockerhoff, E. G. (2014). Pathway-level
551 risk analysis: the net present value of an invasive species policy in the US. *Frontiers in*
552 *Ecology and the Environment*, *12*(5), 273-279.
553
554 12. Hilbert, D. R., Roman, L. A., Koeser, A. K., Vogt, J., & van Doorn, N. S. (2019). Urban
555 tree mortality: a literature review. *Arboriculture & Urban Forestry: 45 (5): 167-200.*, *45*(5),
556 167-200.

557 13. Paap, T., Burgess, T. I., & Wingfield, M. J. (2017). Urban trees: bridge-heads for forest
558 pest invasions and sentinels for early detection. *Biological Invasions*, *19*(12), 3515-3526.
559
560 14. Kovacs, K., Václavík, T., Haight, R. G., Pang, A., Cunniffe, N. J., Gilligan, C. A., &
561 Meentemeyer, R. K. (2011). Predicting the economic costs and property value losses
562 attributed to sudden oak death damage in California (2010–2020). *Journal of*
563 *Environmental Management*, *92*(4), 1292-1302.
564
565 15. Koch, F. H., Ambrose, M. J., Yemshanov, D., Wiseman, P. E., & Cowett, F. D. (2018).
566 Modeling urban distributions of host trees for invasive forest insects in the eastern and
567 central USA: A three-step approach using field inventory data. *Forest Ecology and*
568 *Management*, 417, 222-236.

569 16. Potter, K. M., Escanferla, M. E., Jetton, R. M., & Man, G. (2019). Important insect and
570 disease threats to United States tree species and geographic patterns of their potential
571 impacts. *Forests*, 10(4), 304.

17. McGeoch, M. A., Genovesi, P., Bellingham, P. J., Costello, M. J., McGrannachan, C., & Sheppard, A. (2016). Prioritizing species, pathways, and sites to achieve conservation targets for biological invasion. *Biological Invasions*, *18*(2), 299-314.

18. Sardain, A., Sardain, E., & Leung, B. (2019). Global forecasts of shipping traffic and biological invasions to 2050. *Nature Sustainability*, *2*(4), 274-282.

19. Haack, R. A., Hérard, F., Sun, J., & Turgeon, J. J. (2010). Managing invasive populations of Asian longhorned beetle and citrus longhorned beetle: a worldwide perspective. *Annual review of entomology*, *55*.

20. Lovett, G. M., Weiss, M., Liebhold, A. M., Holmes, T. P., Leung, B., Lambert, K. F., ... & Weldy, T. (2016). Nonnative forest insects and pathogens in the United States: Impacts and policy options. *Ecological Applications*, *26*(5), 1437-1455.

21. Knight, K. S., Brown, J. P., & Long, R. P. (2013). Factors affecting the survival of ash (*Fraxinus* spp.) trees infested by emerald ash borer (*Agrilus planipennis*). *Biological Invasions*, 15(2), 371-383.

22. Fei, S., Morin, R. S., Oswalt, C. M., & Liebhold, A. M. (2019). Biomass losses resulting from insect and disease invasions in US forests. *Proceedings of the National Academy of Sciences*, 116(35), 17371-17376.

23. Kinloch Jr, B. B. (2003). White pine blister rust in North America: past and prognosis. *Phytopathology*, 93(8), 1044-1047.

24. Rizzo, D. M., & Garbelotto, M. (2003). Sudden oak death: endangering California and Oregon forest ecosystems. *Frontiers in Ecology and the Environment*, 1(4), 197-204.

25. Coleman, T. W., Poloni, A. L., Chen, Y., Thu, P. Q., Li, Q., Sun, J., ... *et al.* (2019). Hardwood injury and mortality associated with two shot hole borers, Euwallacea spp., in the invaded region of southern California, USA, and the native region of Southeast Asia. *Annals of Forest Science*, 76(3), 1-18.

26. Coutts, S. R., Helmstedt, K. J., & Bennett, J. R. (2018). Invasion lags: The stories we tell ourselves and our inability to infer process from pattern. *Diversity and Distributions*, 24(2), 244-251.

27. Hijmans, R. J., Phillips, S., Leathwick, J., Elith, J., & Hijmans, M. R. J. (2017). Package 'dismo'. *Circles*, 9(1), 1-68.

28. Fick, S. E., & Hijmans, R. J. (2017). WorldClim 2: new 1-km spatial resolution climate surfaces for global land areas. *International Journal of Climatology*, 37(12), 4302-4315.

29. Homer, C.G., Dewitz, J.A., Yang, L., Jin, S., Danielson, P., Xian, G., … *et al*. (2015.) Completion of the 2011 National Land Cover Database for the conterminous United States – representing a decade of land cover change information. *Photogrammatic Engineering and Remote Sensing,* 81, 345–354.

30. Amodio, S., Aria, M., & D'Ambrosio, A. (2014). On concurvity in nonlinear and nonparametric regression models. *Statistica*, *74*(1), 85-98.

31. Lambert, D. (1992). Zero-inflated Poisson regression, with an application to defects in manufacturing. *Technometrics*, *34*(1), 1-14.

618 32. Wood, S. (2012). *mgcv: Mixed GAM Computation Vehicle with GCV/AIC/REML*
619 *smoothness estimation*. R package.

620 33. Elith, J., Leathwick, J. R., & Hastie, T. (2008). A working guide to boosted regression
621 trees. *Journal of Animal Ecology*, *77*(4), 802-813.

622 34. Aukema, J. E., McCullough, D. G., Von Holle, B., Liebhold, A. M., Britton, K., & Frankel,
623 S. J. (2010). Historical accumulation of nonindigenous forest pests in the continental
624 United States. *BioScience*, 60(11), 886-897.

625 35. Carpenter, B., Gelman, A., Hoffman, M. D., Lee, D., Goodrich, B., Betancourt, M., ... *et al*.
626 (2017). Stan: A probabilistic programming language. *Journal of Statistical*
627 *Software*, 76(1).

628 36. Pugh, S.A. (2010). *Michigan's forest resources, 2008*. Research Note NRS-50. Newtown
629 Square, PA: U.S. Forest Service, Northern Research Station. 4 pp.
630

631 37. Hochberg, M.E., & Weis, A.E. (2001). Ecology: bagging the lag. *Nature* 409, 992–93.

632 38. Liebhold, A.M., & Tobin, P.C. (2008). Population ecology of insect invasions and their
633 management. *Annual Review of Entomology,* 53, 387–408.

Figures and Tables

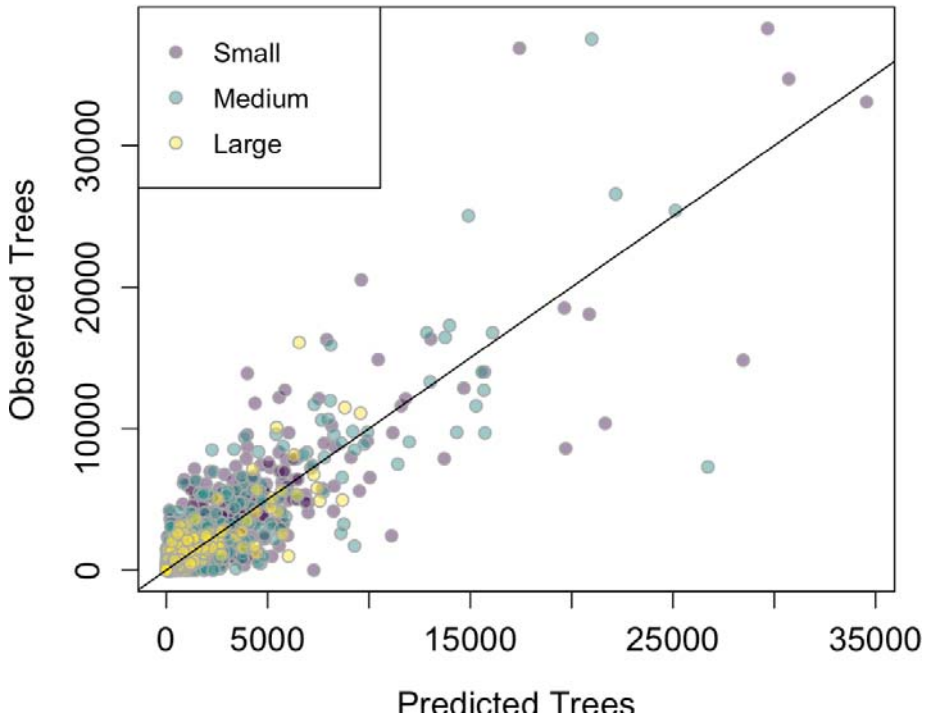

Figure 1. Fit of the genus-specific host tree models across all genera and size classes.

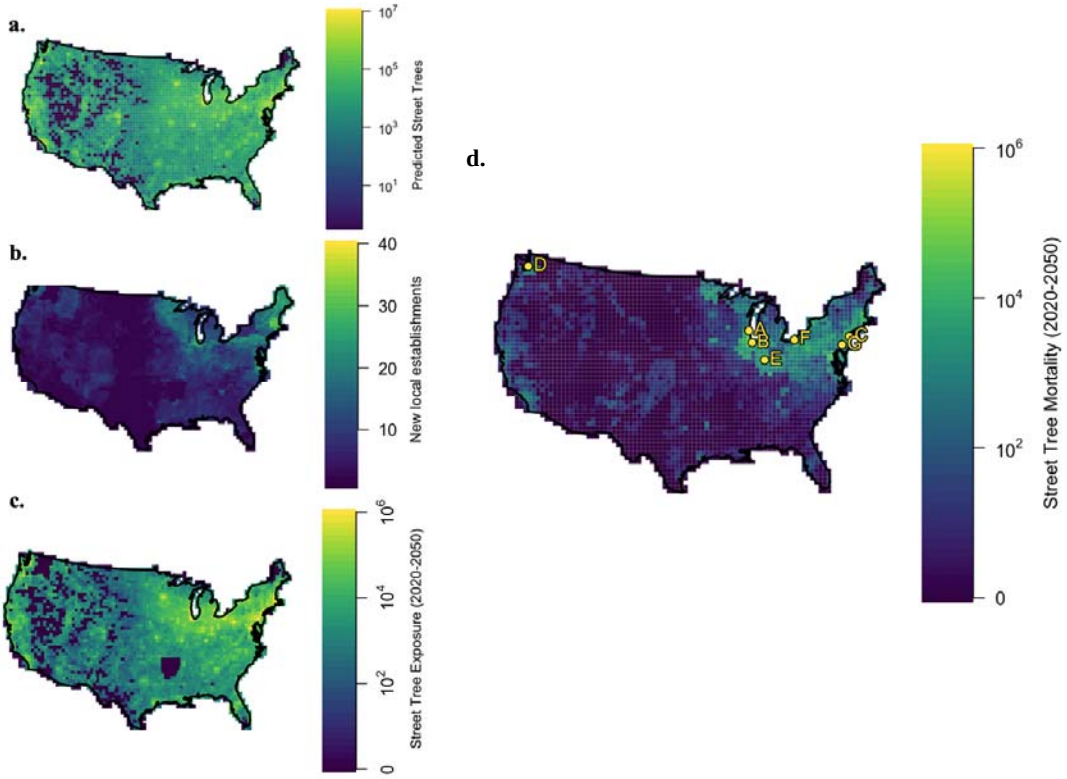

Figure 2. Model outputs for the first three subcomponent models, including **a.** predicted street tree abundance, **b.** predicted newly invaded sites of existing IAFIs, **c.** predicted street tree exposure levels (number of focal host tree + IAFI interactions) from 2020 to 2050, and finally **d.** Predicted total tree mortality from 2020 to 2050 in the most likely mortality debt scenario across space. The top seven most impacted cities or groups of nearby cities are shown in terms of total tree mortality 2020 to 2050 (A = Milwaukee, WI; B = Chicago/Aurora/Naperville/Arlington Heights, IL; C = New York, NY; D = Seattle, WA; E = Indianapolis, IN; F = Cleveland, OH; G = Philadelphia, PA).

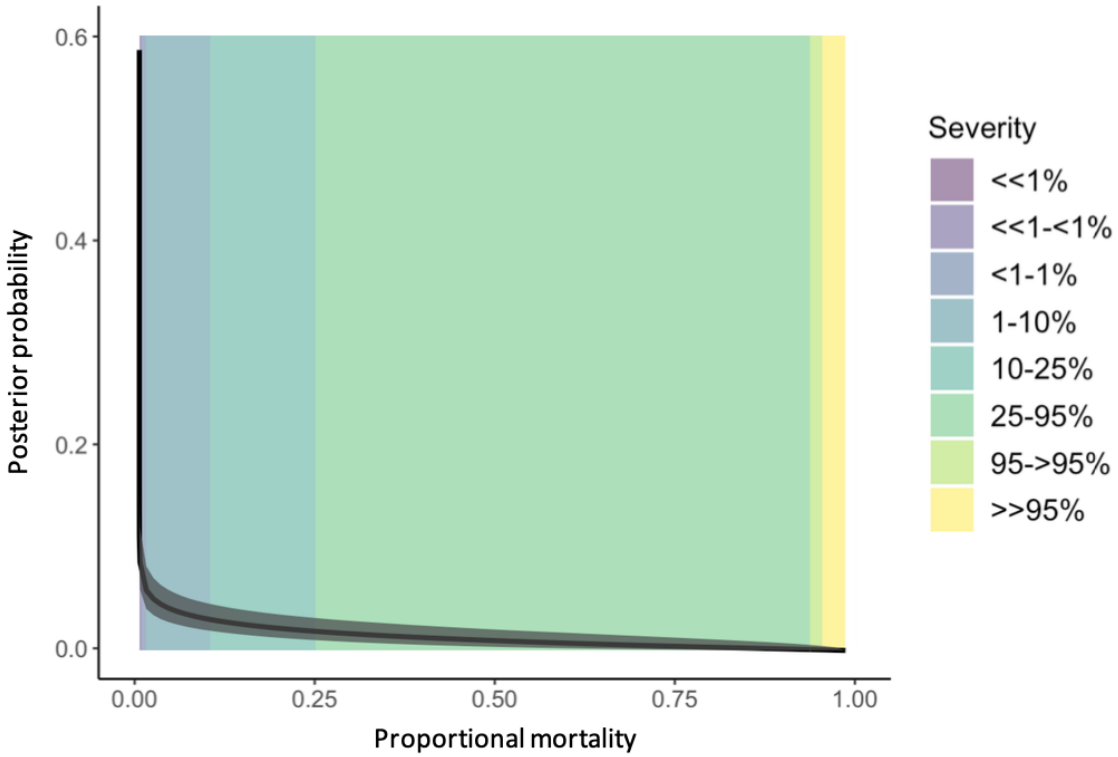

Figure 3. Posterior distribution for the beta model of host mortality due to IAFIs within each severity category. 95% Bayesian credible intervals are shown in grey, and the posterior median is shown in black. Colored bins represent severity categories extended from [14].

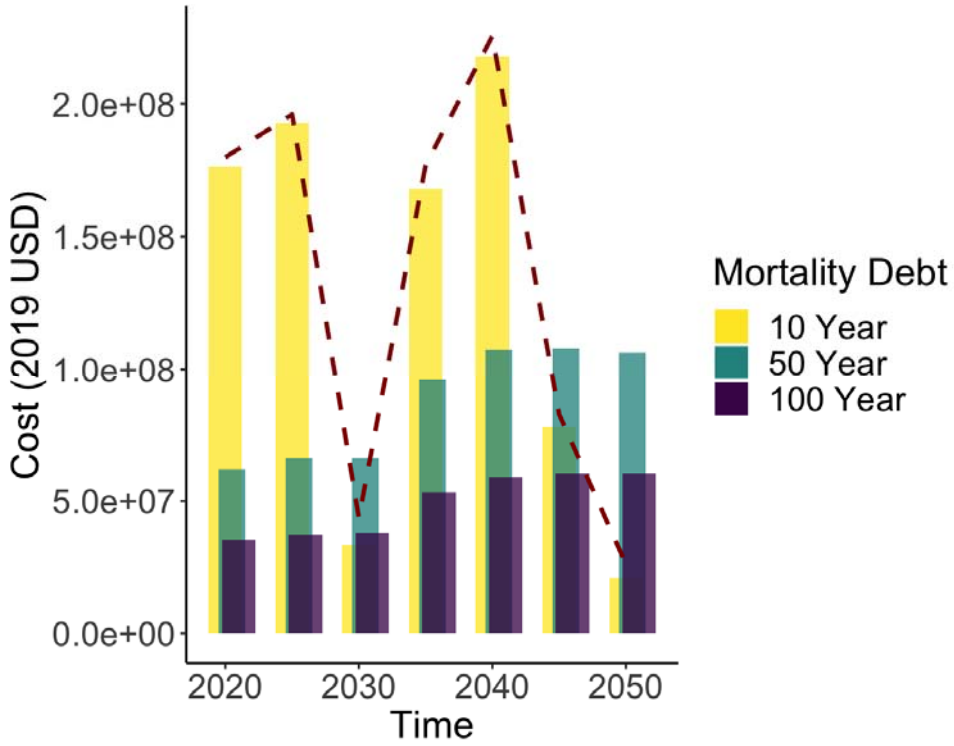

Figure 4. Depiction of the influence of mortality debt on temporal cost patterns. Predicted costs 2020 to 2050 for the 10 year (yellow), 50 year (teal), and 100 year (purple) mortality debt scenarios with a 10 year initial invasion lag. The most likely scenario predictions are shown as a dashed red line. Costs are presented in 5-year increments in accordance with the timestep length within our spread model.

659 **Table 1.** Predicted annualized cost (in 2019 US dollars) and tree mortality across invasion
660 scenarios from 2020 to 2050 across all 57 IAFI species. “Most likely” indicates the scenario with
661 expert-elicited mortality debt durations by feeding guild, “Vary” scenarios hold all guilds but the
662 focal guild constant at their most likely scenario, and “All” fix all three guilds at a given mortality
663 debt duration. Mean mortality for most likely scenario = 2.3%, 1.38M trees, US$ 30M annualized
664 (US$ 679M over the next 30 years).
665

Mortality Debt Scenario	**Annualized Cost (US$ millions)**		**Tree Mortality (Millions)**		**Percent Mortality**	
	lower 95% CI	upper 95% CI	lower 95% CI	upper 95% CI	lower 95% CI	upper 95% CI
Most likely	28.5	33.2	1.29	1.54	2.1%	2.5%
Vary Borers	10.1	32.1	0.45	1.45	0.7%	2.4%
Vary Defoliators	28.1	32.6	1.28	1.48	2.1%	2.4%
Vary Sap-feeders	28.5	32.5	1.30	1.47	2.1%	2.4%
All 10	27.8	30.4	1.27	1.39	2.1%	2.3%
All 50	18.5	22.3	0.84	1.00	1.4%	1.7%
All 100	9.77	13.5	0.44	0.60	0.7%	1.0%

666